Effects of uncertainties and soil heterogeneity on the seismic response of archaeological areas: a case study

Alessandro Pagliaroli,* Massimiliano Moscatelli,* Giuseppe Scasserra,*
Giuseppe Lanzo,** Giuseppe Raspa***

Summary

The paper deals with a numerical study aimed at the evaluation of the seismic response of the Central Archaeological Area of Rome including Palatine hill, Roman Forum, and Coliseum. A relevant role is played by buried morphology and mechanical properties of the anthropogenic cover which reaches a thickness of 20 m. This layer is constituted by "dominant masonry" and "dominant infill" zones strongly variable in the space thus exhibiting wide spatial heterogeneity in dynamic properties whose definition is affected by high degree of uncertainty. In order to investigate the effects of the uncertainty in dynamic soil properties of the anthropogenic unit on ground motion at surface, 1D and 2D stochastic analyses were carried out. The numerical results were then compared with those obtained from a standard deterministic model defined by using "average" values of dynamic properties.

The influence of uncertainty in shear wave velocity distribution as well as in nonlinear properties (i.e. normalized shear modulus and damping curves) of the anthropogenic cover is highlighted in terms of Housner Intensity amplification factors profiles and acceleration response spectra in representative nodes at surface.

1. Introduction

The numerical modeling of site response requires a subsoil model (*i.e.*, definition of soil stratigraphy and physical/mechanical characterization of lithotypes) and specification of an input motion. Site response analyses are usually performed in a deterministic way: mean values of the physical and mechanical properties are assumed for each homogenous layer indentified in the subsoil model while a number of rock motion time histories, fitting on average a reference spectrum, are assumed as input motion.

This approach, however, does not allow the assessment of variability of ground motion due to uncertainty associated to the process. In particular four basic sources of uncertainty affect the results of a numerical site response analysis [Idriss, 2004; Rathje *et al.*, 2010]: 1) specification of the input rock motions; 2) characterization of the shear-wave velocity profile; 3) characterization of the nonlinear soil properties; and 4) selection of the method of analysis (i.e. 1D/2D/3D geometry of the analysis and constitutive models of the soils). Point 2 and 3 refers to the subsoil model whose uncertainty is affected by a combination of epistemic (lack of knowledge) and aleatory uncertainty (related to the intrinsically stochastic nature of model parameters) [Rota *et al.*, 2011].

Starting from Faccioli [1976], several studies in the literature have focused on site property uncertainty (*e.g.* Rathje *et al.*, 2010; Andrade and Borja, 2006 and reference therein), essentially in 1D conditions and with a statistical analysis of the Monte Carlo type. Some Authors considered only some of the sources of uncertainty while other (*e.g.* Rota *et al.*, 2011) proposed fully probabilistic procedures to take into account at the same time the uncertainty associated to all factors driving site response: stratigraphy, Vs distribution, non linear properties and input motion.

The analyses presented in this paper cannot be regarded as fully stochastic site response analyses since the goal of the study is to highlight the role of uncertainty in dynamic properties of a thick anthropogenic cover on site response results at ground surface in the case of an archaeological area. The selected case study is the Central Archeological area of Rome which includes Palatine Hill, Roman Forum, and Coliseum. The study was performed in the framework of a larger research project, sponsored by the Italian Department of Civil Protection, aimed at geohazard assessment affecting the area [Cecchi 2010, 2011; Moscatelli *et al.*, 2014a]. A "deterministic" subsoil model for the site response analyses was built by integrating all the available information with the results of a new survey carried out in 2010-2011 including continuous-coring boreholes, in situ and laboratory geotechnical tests, MASW, Cross- and Down-Hole tests, ambient noise measurements, electrical resisti-

* CNR-IGAG, Istituto di Geologia Ambientale e Geoingegneria
** Dipartimento di Ingegneria Strutturale e Geotecnica, Sapienza Università di Roma
*** Dipartimento di Ingegneria Chimica Materiali Ambiente, Sapienza Università di Roma

vity tomographies, ground penetrating radar surveys [Moscatelli *et al.,* 2012; Pagliaroli *et al.,* 2014a]. For the definition of the subsoil model particular efforts were devoted to the characterization of the buried morphology and the mechanical properties of the anthropogenic cover. The thickness of the cover reaches 20 m and therefore strongly controls the seismic response in the moderate-to -high frequency range. Moreover this layer is constituted by "dominant masonry" and "dominant infill" zone highly variable in the space thus exhibiting wide spatial heterogeneity in dynamic properties.

Starting from in-hole tests carried out in the anthropogenic cover, 2D geostatistical conditional simulations of shear wave velocity were carried out and used for 2D stochastic site response analyses. Moreover, the influence of uncertainty in both shear-wave velocity profile and nonlinear properties (*i.e.* normalized shear modulus and damping curves) of the anthropogenic cover was assessed through 1D Monte Carlo simulations, at selected vertical profiles. Both 1D and 2D numerical simulations of site response were performed using equivalent linear model considering the moderate seismicity on the area and because this method of analysis is most common in practice.

At the end of the study we quantified how modeling soil property variability in highly heterogeneous soils (like anthropogenic cover in archaeological areas and ancient urbanized areas) influences amplification factors and response spectra with respect to standard deterministic estimates.

2. Geological and morphological setting

The natural landscape of the Palatine hill has been completely modified by human reworking over the last thousand years. However, referring to the hills of the present day Roman countryside as an analogue, the original topography of the Palatine hill can be inferred: an almost flat plateau bordered by steep slopes and surrounded by narrow and elongated alluvial valleys.

A thick deposit of anthropic origin, which locally reaches 20 m in thickness, presently covers the study area. The few geological outcrops are visible only where natural substratum is made exposed by archaeological excavations, or where this substratum was not covered by artificial structures [Pensabene 2001; Tomei and Filetici, 2011]. Therefore, the geological and morphological settings of the hill were mainly assessed making reference to the geological literature and using over 200 geotechnical boreholes available from vintage and new drilling campaigns (Fig. 1).

The Plio-Pleistocene sandy marly marine sediments of the Monte Vaticano Formation [Funiciello and Giordano, 2008] constitute the geological bedrock of the study area [Moscatelli *et al.*, 2012; Mancini *et al.*, 2014]. Middle Pleistocene interstratified sedimentary (fluvial-palustrine) and volcanic (tuffs) units overly the geological bedrock and constitute the framework of the Palatine hill [Mancini *et al.*, 2014].

The recent hydrographic network deeply carved the Pliocene-Pleistocene units during the last sea-level fall (Late Quaternary), giving rise to narrow alluvial valleys: Velabro, Labicano, and Murcia valleys (Figs. 1, 2).

Finally, anthropogenic covers buried the Late Quaternary alluvial valleys as well as the previous geological units. Integration of archaeological information, stratigraphies from boreholes, ERT, and GPR data (Fig. 3) allowed us to define the main lithological "signatures" of the anthropogenic covers and define homogeneous zones that are relevant for the evaluation of local seismic response [Moscatelli *et al.,* 2014b]: (i) zones with dominant masonry remains, and (ii) zones with dominant infill. These zones are distributed patchily and extremely complex in terms of their internal geometries and nature of materials involved.

Zones characterized by dominant masonry consist predominantly of masonry fragments and building remains (generally brick walls) that are still rooted on their foundations (mainly concrete with inert basalt and brick materials). The thickness the anthropogenic unit in correspondence of these zones locally exceeds 15 m and they are extended laterally for tens of meters. The building remains, which show different levels of preservation, typically alternate with sandy-pebbly fill materials (primarily fragments of bricks, ceramics and pottery) immersed in a silty-clay or pozzolan matrix.

Zones with dominant infill are generally subordinate and are usually located on top of building remains. Fill materials consist of sandy-pebbles (fragments of bricks, ceramics and pottery) in a silty-clay or pozzolan matrix; the fine-grained fraction is locally dominant.

The integration of ERT (Electrical Resistivity Tomography) and GPR (Ground Penetration Radar) surveys, which were calibrated and constrained using geological cross-sections in addition to borehole and archaeological stratigraphies, also allowed us to rigorously reconstruct the morphology buried below the anthropogenic layer. On this regard, the basal surface of the anthropogenic covers was interpolated by means of multicollocated cokriging, and the thickness of this unit was then calculated starting from a DTM (Digital Terrain Model) having a spatial resolution of 3x3 m and the interpolated basal surface of the anthropogenic layer [Moscatelli *et al.,* 2014b]. A full description of the methodology used for interpolating the target surface is beyond the scope of this paper and the reader is referred to Chilès

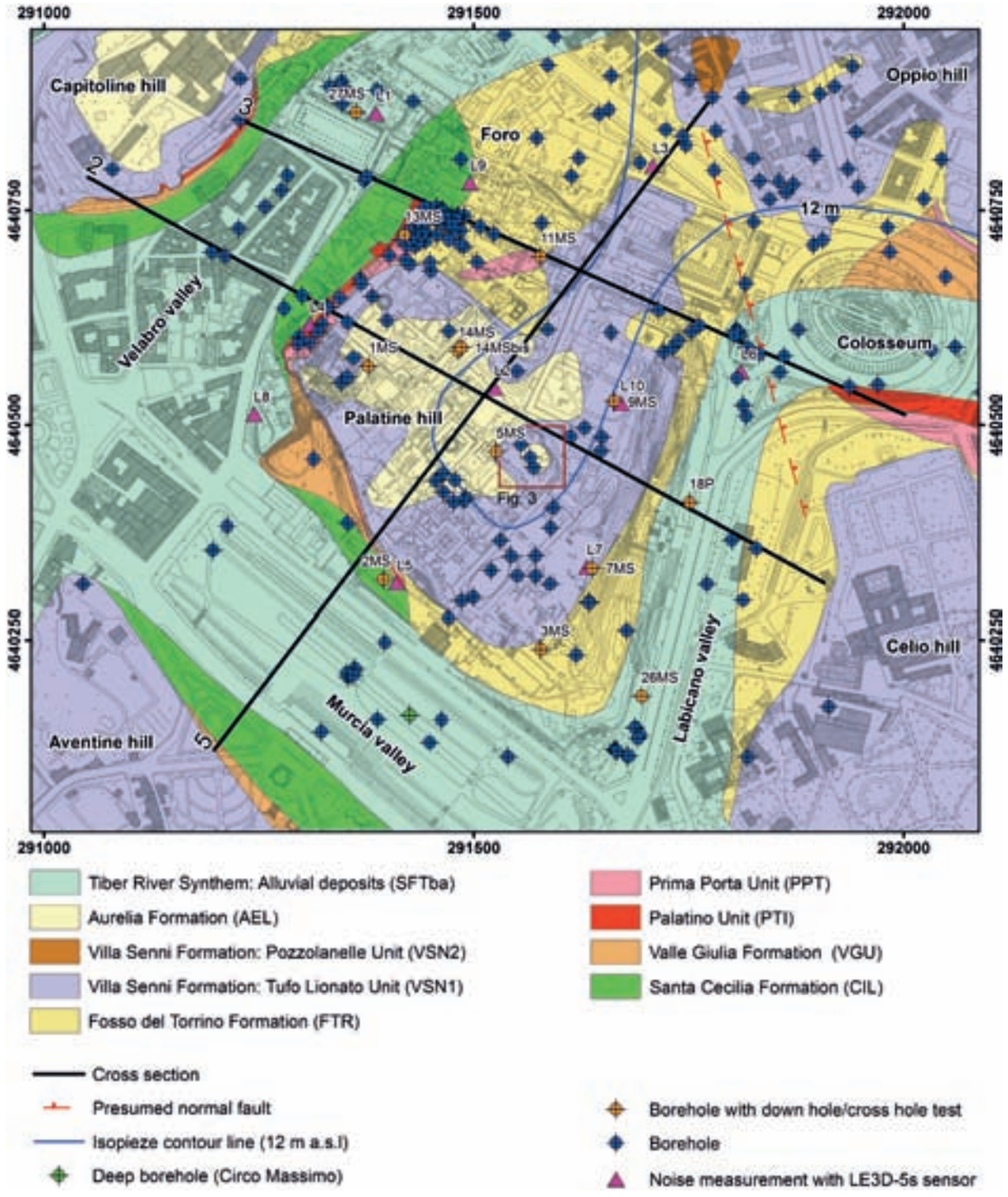

Fig. 1 – Geological map of Central Archeological Area of Rome showing the location of boreholes, noise measurements and geological cross-sections of Fig. 2. The location of Fig. 3b is also indicated (modified after MANCINI *et al.*, 2014).
Fig. 1 – Carta geologica dell'Area Archeologica Centrale di Roma che mostra le posizioni dei sondaggi, delle misure di rumore ambientale e dei profili geologici di Fig. 2. In figura è indicata anche la localizzazione della Fig. 3b.

and DELFINER [1999] and MOSCATELLI *et al.* [2014b] for details.

The general morphology reconstructed by interpolating available data includes three main valleys bounding the Palatine hill to the West, East, and South (Velabro, Labicano, and Murcia, respectively; see Fig. 4), and a saddle to the North (*i.e.*, the Velia hill), connecting the Palatine and Oppio hills [MOSCATELLI *et al.*, 2014b].

When looking in detail at the buried morphology it is evident that geology played a fundamental role in conditioning the final shape of the contact betwe-

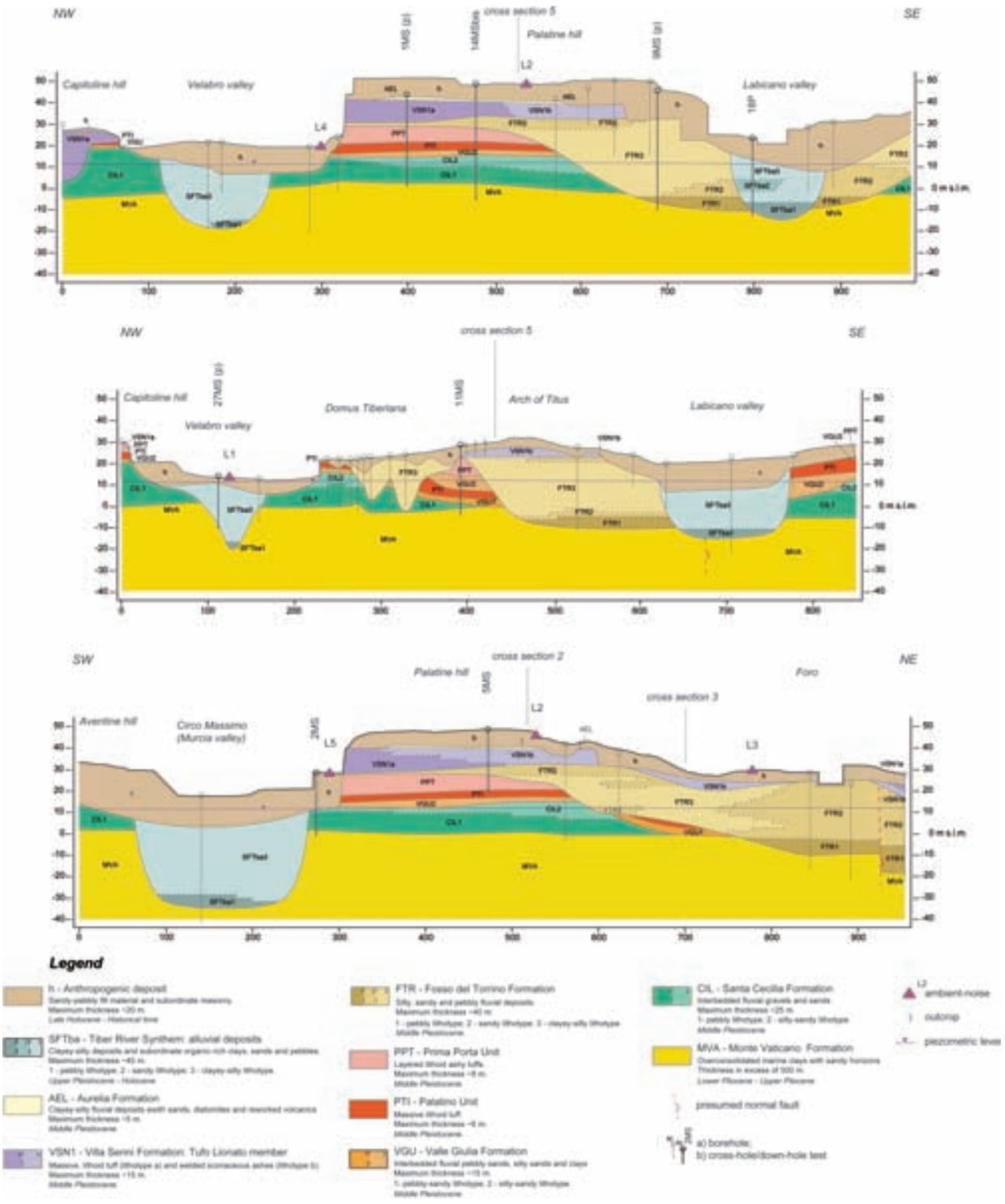

Fig. 2 – Geological cross-sections of the Central Archaeological Area of Rome, with indication of the lithotypes. For location of cross-sections, see Fig. 1 (modified after MANCINI *et al.*, 2014).

Fig. 2 – Profili geologici dell'Area archeologica Centrale di Roma, con indicazione dei litotipi. Per la traccia dei profili, vedi Fig. 1.

en anthropogenic and natural layers. As a matter of fact, the complex geological setting is reflected in the morphological features bounding the flanks of the hill: 5-10 m high escarpments cut the tuffs overlooking the Velabro and Murcia valleys, while more gentle clayey slopes join the hilltop plateau with the Labicano valley to the east and the Oppio hill to the north. Except for a few outcrops, most of which are located

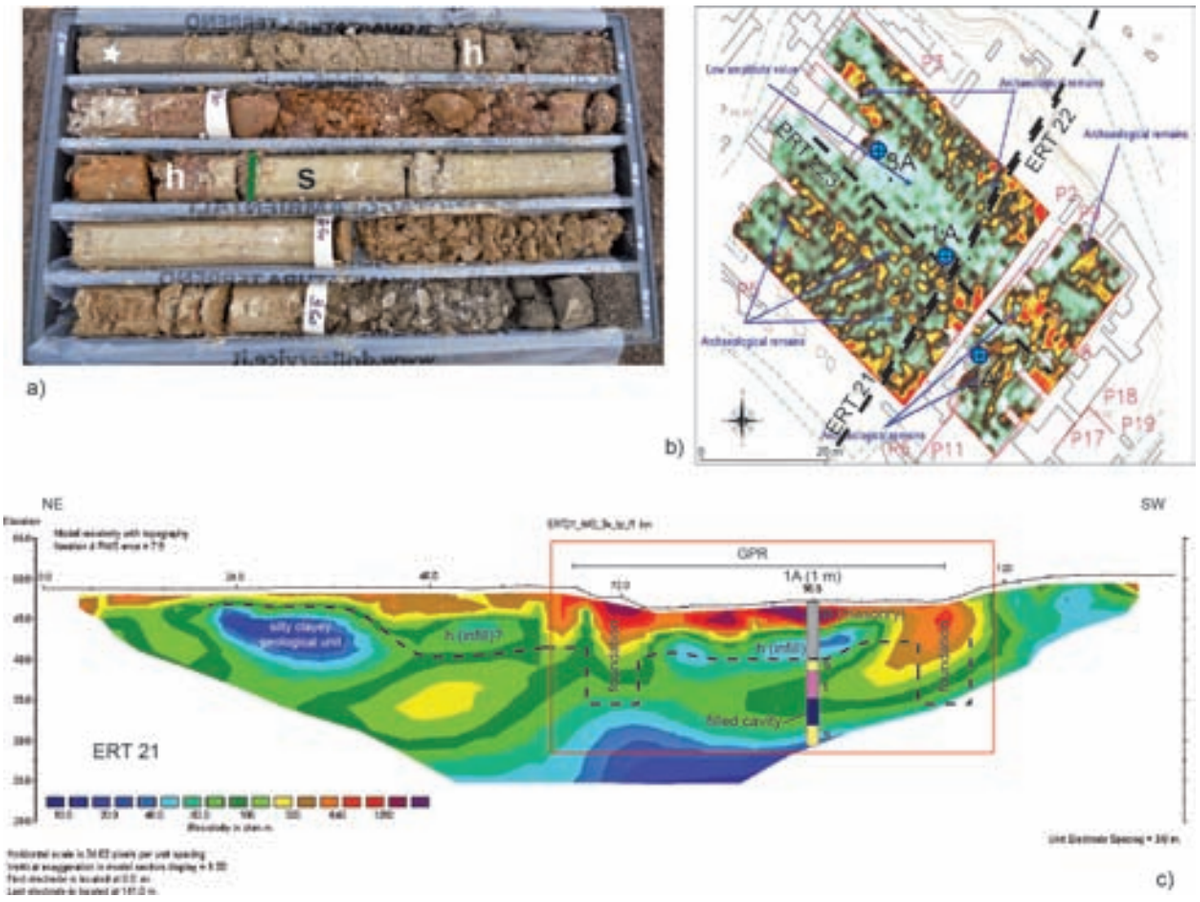

Fig. 3 – a) Core of the archaeological layer (h) from borehole 1A (well-head elevation 47 m a.s.l.), between 5 and 10 m (a) from the well-head: weathered brick wall, infill material, and silty clays derived from excavation of geological materials (white star) are visible - the contact (green line) with the geological bedrock (s, sedimentary deposits) is also visible; b) example of GPR amplitudes map for 35 MHz antennas, at the averaged estimated depth of 6 m from ground surface, showing a NW-SE trending, low-amplitude zone (infill material) surrounded by medium to high-amplitude reflectors referable to archaeological remains - tracks of ERT 21, ERT 22, and ERT 23 and position of boreholes 1A, 2A, and 3A are also reported; c) ERT 21 with interpretation of the probable contact between archaeological and geological layers (dashed black line) - the red box indicates the Peristyle of the Domus Augustana, where the log of geotechnical borehole 1A (in brackets the distance of projection in meters; h, s, and t indicate the archaeological layer, the sedimentary deposits, and the tuffs, respectively) and the extension of the GPR survey are reported. Note that the depth of foundations in c) is constrained via borehole 5MS (see Fig. 1 for location) (modified after Moscatelli *et al.*, 2014b)
Fig. 3 – a) Carota del livello archeologico (h) del sondaggio 1A (quota boccapozzo 47 m s.l.m.), tra 5 e 10 m dal piano campagna: sono visibili murature in mattoni alterate, materiale di riempimento e argille siltose derivanti dall'escavazione dei materiali geologici (stella bianca) - in evidenza il contatto (linea verde) con il substrato geologico (s, depositi sedimentari); b) esempio di mappa GPR relativa alle acquisizioni con antenna da 35 MHz, ad una profondità media stimata di 6 m dal piano campagna, che mostra una zona caratterizzata da riflettori a bassa ampiezza (riempimenti), con andamento NO-SE, circondata da riflettori a media e alta ampiezza riferibili a resti archeologici - sono riportate anche le tracce delle ERT 21, ERT 22 e ERT 23 e le posizioni dei sondaggi 1A, 2A e 3A; c) ERT 21 con interpretazione del possibile contatto tra substrato geologico e livello archeologico (linea nera tratteggiata) - il Peristilio della Domus Augustana è indicato nel riquadro rosso, all'interno del quale è riportata la traccia del sondaggio 1A (tra parentesi la distanza di proiezione in metri; h, s, t indicano rispettivamente il livello archeologico, i depositi sedimentari e i tufi) e l'estensione del rilievo GPR. Notare che la profondità delle fondazioni in c) è vincolata con il sondaggio 5MS (vedi Fig. 1 per la posizione).

along the western side of the hill, these features are buried by the anthropogenic layer. The present day setting of this layer is the result of the superimposition of structures, cuts, excavations, and fillings that produced a final aggradation of the hilltop of 5-10 m (Figs. 3 and 4) and a lateral accretion of the hill flanks because of the substructures. Where these lateral growths involved the steep volcanic slopes, space for new buildings was also created by removing up to 10 m in thickness of tuffs, especially the uppermost volcanic unit of the hill, and creating flat terraces (see the southern slope of the hill in Fig. 4).

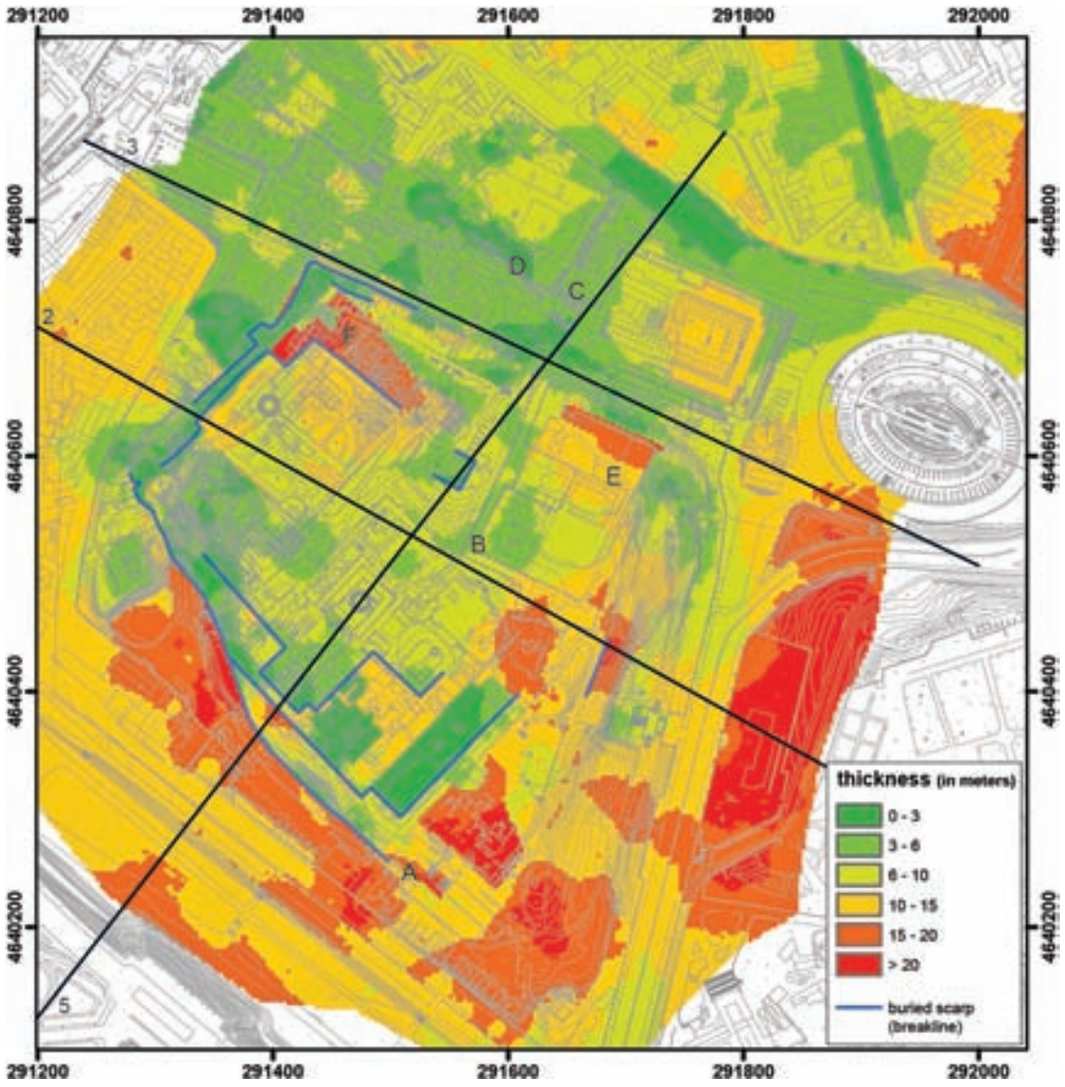

Fig. 4 – Raster map of the thickness of the anthropic layer (blue lines indicate the paths of the escarpments used as break lines for the interpolation). Legend of localities: A), Schola Praeconum-Arcate Severiane; B), Peristyle of the Domus Augustana; C), Santa Maria Nova; D), Via Sacra; E), Vigna Barberini; F), Domus Tiberiana. Note that thickness of the anthropic layer was not calculated at the Colosseum because no DTM was available at that location. The tracks of the geological cross-sections of Fig. 2 are also indicated (modified after MOSCATELLI *et al.*, 2014b).

Fig. 4 – Mappa raster dello spessore del livello antropico (le linee blu indicano le tracce delle scarpate usate con linee di interruzione per l'interpolazione). Legenda dei luoghi: A), Schola Praeconum-Arcate Severiane; B), Peristilio della Domus Augustana; C), Santa Maria Nova; D), Via Sacra; E), Vigna Barberini; F), Domus Tiberiana. Notare che lo spessore del livello antropico non è stato calcolato per il Colosseo, dove manca un DTM di riferimento. Le linee nere indicano le tracce dei profili geologici di Fig. 2.

3. Subsoil model

3.1. Identification of seismic bedrock

The overconsolidated clays of the Monte Vaticano Formation have an average shear wave velocity (V_S) lower than 500 m/s in the upper tens of meters, as determined by direct geophysical tests [PAGLIAROLI *et al.*, 2014a]. This value is quite smaller than the 800 m/s usually assumed for seismic bedrock during site response analyses. A noise measurements campaign was therefore undertaken to identify the depth of seismic bedrock [PAGLIAROLI *et al.*, 2014b]. Microtremor measurements were performed at 10 sites located throughout the study area (see Fig. 1 for location) using 5 seconds 3-component Lennartz® velocity transducer (LE3D-5s). All the measurements showed a clear H/V peak around 0.3-0.35 Hz, thus suggesting the presence of a several hundred meters deep seismic bedrock.

The seismic bedrock position was therefore identified by considering: i) a very deep well located

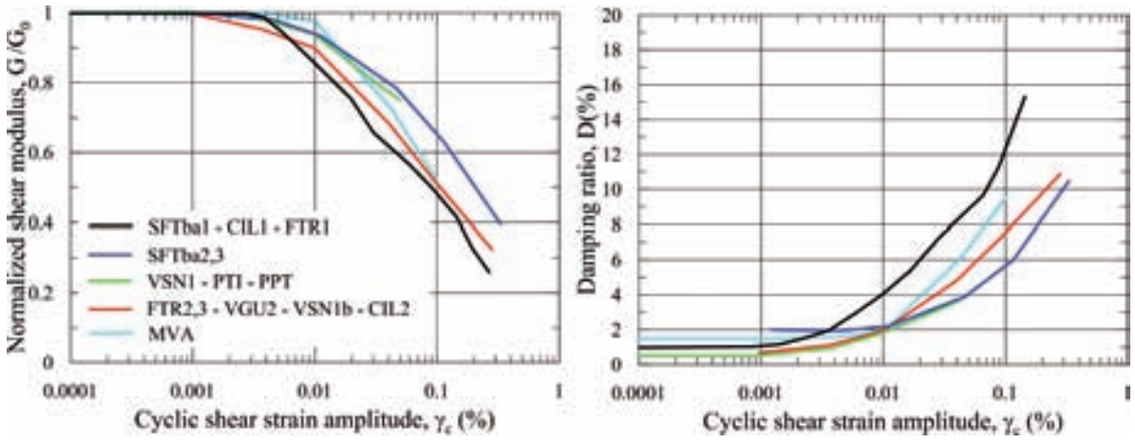

Fig. 5 – Non-linear behaviour of soils and soft rocks: $G(\gamma_c)/G_0$ and $D(\gamma_c)$ curves selected for each lithotype and assumed in the integrated subsoil model for site response analyses.

Fig. 5 – Caratterizzazione del comportamento non lineare dei terreni e delle rocce tenere ai fini delle analisi di risposta sismica locale: curve $G(\gamma_c)/G_0$ e $D(\gamma_c)$ selezionate per ciascun litotipo.

in the Circo Massimo (Deep borehole Circo Massimo in Fig. 1), crossing the entire 900 m thick MVA Formation and intercepting the passage between the clayey lithotype and the underlying stiffer sandy-clayey lithotype at about 560 meters from the ground surface [SIGNORINI, 1939]; ii) the results of 1D parametric site response analyses aimed at reproducing the site fundamental frequency at 0.30-0.35 Hz. According to these analyses, the V_S-depth profile best matching the experimental results shows a V_S average value of 550 m/s in the upper 200 m of the MVA Formation, 600 m/s in the subsequent 200 m, and 650 m/s in the lower 100 m of the MVA; the value $V_S \geq 800$ m/s (*i.e.* seismic bedrock) occurs below a depth of 500 m from the top of the MVA Formation, in substantial agreement with the Circo Massimo borehole [PAGLIAROLI *et al.*, 2014b].

3.2. Characterization of pre-anthropic units

The site response analyses here conducted adopt the traditional visco-elastic linear-equivalent approach. As such, the subsoil numerical model requires the characterization of each unit in terms of unit weight (γ), shear wave velocity (V_S), compression wave velocity (V_P) or, similarly, Poisson ratio (ν); the variation of normalized shear modulus (G/G_0) and damping ratio (D) with shear strain amplitude (γ_c) is also required. The S-wave velocities were determined for the study area from a total of 17 Cross-Hole (CH) tests, 11 Down-Hole (DH) tests, 3 Seismic Dilatometer (SDMT) tests, and 20 MASW tests available from existing studies as well as the newly conducted 2010 survey [PAGLIAROLI *et al.*, 2014a]. Each lithotype was therefore characterized by averaging V_S and V_P across the different depth ranges. A constant value of the geophysical parameters with depth was therefore assumed with exception of the anthropogenic layer (h) and the MVA, for which a V_S gradient with depth was defined. For lithotype h the gradient was derived by interpolating all available measurement points as shown later while, as said before, for the MVA a V_S trend was deduced by reproducing the experimental site fundamental frequency using 1D analyses.

The normalized shear modulus $G(\gamma_c)/G_0$ and the damping ratio $D(\gamma_c)$ variation with shear strain amplitude were measured from a total of 20 resonant column and 2 cyclic torsional shear tests available from previous surveys in the area, as well as from results of 12 new cyclic simple shear tests performed in 2010-2011. As reported in details by PAGLIAROLI [2014a], in these latter tests particular attention was given to those which had not been investigated in previous surveys (mainly organic clays SFTb3 and tuffs PTI-PPT-VSN1a). For gravelly soils (CIL1, FTR1 and SFTba1), for which undisturbed sampling was not possible, reference was made to literature data obtained on materials having a similar granulometric distribution [HATANAKA *et al.*, 1988]. Where multiple laboratory determinations for the same lithotype were available, the average range of the $G(\gamma_c)/G_0$ and $D(\gamma_c)$ curves obtained at in situ confining pressure was used. Only for the MVA marly member, considering its significant thickness (about 500 m), the laboratory cyclic simple shear curves at the highest confirming pressure applicable in the test apparatus were preferred [PAGLIAROLI *et al.*, 2014a].

Finally the lithotypes were grouped into sets characterized by similar values for the properties relevant for site response analyses: unit weight γ, V_S, ν and $G(\gamma_c)/G_0$ and $D(\gamma_c)$ curves. The physical and mechanical properties adopted for the subsoil model are summarized in table I and figure 5.

Tab. I – Integrated subsoil model for site response analyses. Legend: γ=unit weight, V_S=shear wave velocity, ν=Poisson ratio. See legend of Fig. 2 for a description of the lithotypes. * gradient with depth.
*Tab. I – Modello integrato di sottosuolo utilizzato per le analisi di risposta locale. Legenda: γ = peso dell'unità di volume, V_S=velocità delle onde di taglio, ν=coefficiente di Poisson. Vedere la legenda di Fig. 2 per la descrizione dei litotipi. * gradiente con la profondità.*

Lithotype	γ (kN/m^3)	V_S (m/s)	ν(-)
h	18.0	$V_S=185z^{0.31}$	0.42
SFTba2,3	18.5	270	0.49
SFTba1	20.0	590	0.46
VSN1a	16.0	600	0.40
PTI-PPT	16.0	650	0.39
FTR2,3-VGU2-VSN1b-CIL2	19.7	340	0.48
VGU1	20.0	390	0.42
FTR1	20.5	680	0.45
CIL1	20.5	620	0.39
MVA	20.5	550-650*	0.48
Seismic bedrock	22.0	800	0.46

3.3. Characterization of the anthropic unit

The anthropogenic layer (h), generally formed by soil of variable grain size and masonry with extremely variable weathering, exhibits a wide spatial heterogeneity and a significant stiffness gradient with depth. Given the close spatial continuity of the various components (soil, masonry, underground cavities, foundations), it was not possible to identify macroareas characterized by homogeneous composition and stiffness. For this reason MASW tests proved particularly useful in that they sample a larger volume of the subsurface as compared to borehole seismic methods providing "average" values of material properties. In-hole tests sample a smaller volume of material and therefore provides a more localized measure of material properties. As a matter of fact, V_S data obtained from some DH tests are quite scattered around the average trend provided by MASW. In this respect, the average value (m) and standard deviation (σ) of V_S were computed at each depth (z) from ground surface utilizing all in-hole and MASW tests. Down-hole V_S profiles falling outside the range m-σ/m+σ were excluded. New average and average ±1 standard deviation profiles as well as a V_S-z relationship obtained by fitting the remaining data with an exponential function ($V_S=185\times z^{0.31}$) were computed (Fig. 6a). The excluded DH measurements generally correspond to tests involving foundation structures.

The exponential function was then adopted for the whole studied area in the numerical analyses carried out with the deterministic model while m±σ profiles were employed to constrain the 1D stochastic analyses as discussed later.

Regarding the nonlinear behaviour, given the prevalence of coarse material in the composition of the anthropogenic layer, reference was made to the curves proposed by ROLLINS *et al.,* [1998] for gravelly soils. The Authors collected experimental data on a wide variety of gravels, thus allowing to define the mean curve and ± one standard deviations bounds (Fig. 6b). The average data were employed for deterministic 1D and 2D equivalent linear analyses while the range delimited by standard deviations bounds was implemented in 1D stochastic equivalent linear analyses as discussed later in the text.

4. Definition of input motion

The monumental heritage of Rome has undoubtedly been subjected to earthquake-induced damage: the macroseismic intensity in Rome has reached VII MCS on at least six different occasions in the past [GALLI and MOLIN, 2014]. Rome is affected by earthquakes associated with three different seismogenic districts: 1) the seismogenetic structures of the Central Apennine mountain chain, located about 90-130 km east of Rome, responsible for events having a magnitude M of up to 6.7-7.0; 2) the Colli Albani volcanic area, located 20 km to the south of the city (M=5.5); 3) the Rome area itself (inside the beltway, *i.e.*, the Grande Raccordo Anulare) characterized by rare, shallow, low-magnitude events (M < 5).

SABETTA [2014] used both probabilistic and deterministic seismic hazard assessment techniques to evaluate the seismic input for site response analyses. Among the different Uniform Hazard Spectra (UHS) considered for the probabilistic approach, the INGV UHS with a return period of 475 years and rock site conditions was selected (Fig. 7). It should be noted that this spectrum essentially corresponds to the Italian National Building Code spectrum (*i.e.*, the Norme Tecniche per le Costruzioni; NTC-08), which was based on the INGV study. The INGV UHS spectrum was then used to simulate a spectrum-compatible time-history acceleration with the software Belfagor [MUCCIARELLI *et al.,* 2004].

The probabilistic approach, using the INGV UHS spectrum, was employed for site response analyses aimed at defining the microzonation maps of the area [PAGLIAROLI *et al.,* 2014c]. This is because microzonation is essentially a planning tool focused on preventing damage that could occur due to future earthquakes having different magnitudes and distances from the site. In this respect, the probabilistic approach is certainly more suitable [ANSAL *et al.,* 2009] as it allows to construct an equi-probable spectrum combining a series of earthquakes that can affect, to different degrees, the study site.

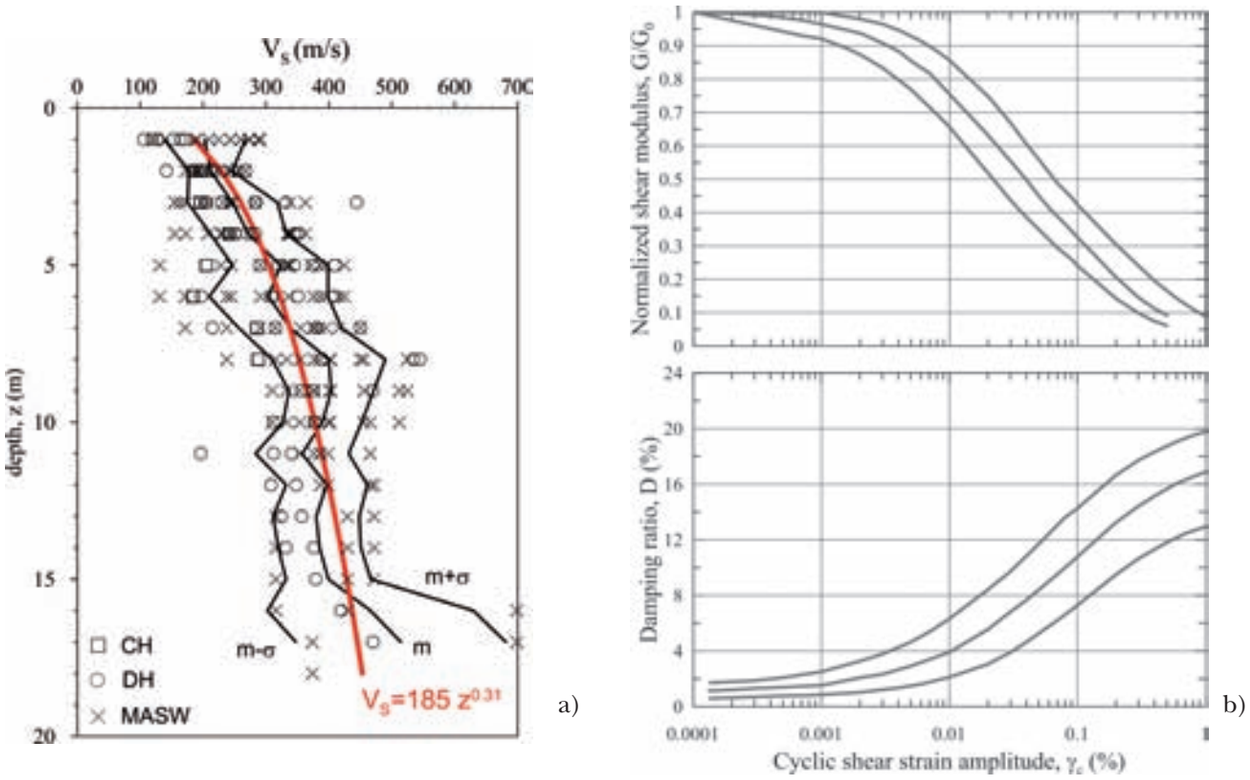

Fig. 6 – a) Vs trend with depth in the anthropogenic layer from in-hole and surface wave tests: average (m) and average ± 1 standard deviation (m ± σ); the best fitting exponential curve is also shown; b) average and average ± 1 standard deviation curves proposed by ROLLINS *et al.,* [1998] for gravelly soils and adopted for non linear behaviour modelling of anthropogenic unit.

Fig. 6 – a) Andamento della V_S con la profondità nello strato antropico con indicazione dei valori medi (m) e medi ± 1 *standard deviation (m ± σ); è mostrato inoltre anche il profilo ottenuto interpolando i dati con una legge esponenziale; b) curve medie e medie* ± 1 *standard deviation proposte da* ROLLINS et al., *[1998] per terreni ghiaiosi ed adottate per la modellazione del comportamento non lineare dello strato antropico.*

Also in numerical simulations carried out in the present study, the INGV UHS spectrum-compatible time-history acceleration was employed. In the present study uncertainty in input motion was therefore neglected even if some studies [*e.g.,* BAZZURRO and CORNELL, 2004] showed that the variability introduced by the input motions was more important than the variability introduced by soil property uncertainties.

However, with reference to the Central Archaeological Area of Rome, PAGLIAROLI *et al.,* [2014b] carried out analyses using other accelerograms besides the INGV UHS spectrum-compatible time-history acceleration, in order to assess the sensitivity of site response to different input motions. In particular the Authors employed natural and artificial accelerograms compatible with the two main deterministic scenarios identified by SABETTA [2014]: 1) Colli Albani volcanic complex, with Mw=5.5 and an epicentral distance of R=20 km; 2) Fucino basin source (Mw=7.0, R = 85 km) (Fig. 7).

PAGLIAROLI *et al.,* [2014b] found that the amplification factors associated with the different input motions agree from both a qualitative and quantitative point of view in all the period ranges. Only in limited portions of the area differences as high as 30-40% were observed. The Authors ascribed this behaviour to the moderate nonlinearity experienced by the soils.

5. Numerical analyses: codes and methodologies

For the seismic microzonation of the area PAGLIAROLI *et al.,* [2014c] employed the results of 2D numerical analyses carried out on 7 cross sections characterized by the deterministic model reported in table I and figure 5.

In the present study in order to investigate the effects of uncertainties in dynamic properties of the anthropogenic unit on site response, reference was made to cross-section #2 cutting the Palatine Hill through its centre in a NW-SE direction (see trace in Fig. 1); this section can be considered as representative of the morphological, geological and mecha-

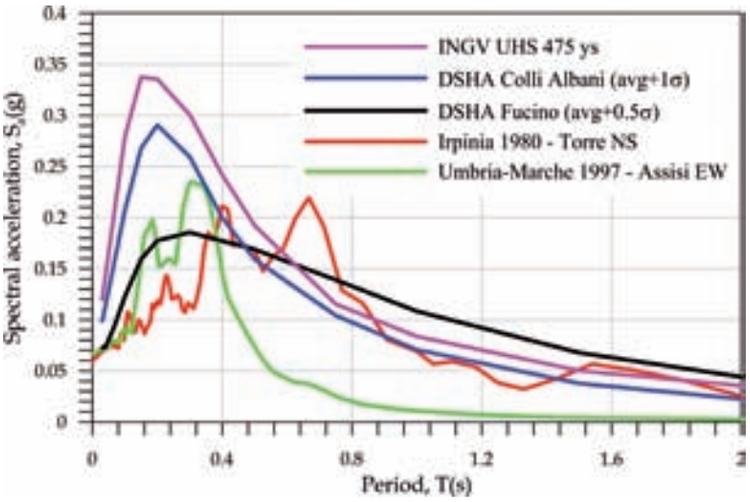

Fig. 7 – Reference spectra selected for the seismic microzonation of the Central Archaeological Area of Rome from probabilistic (INGV UHS) and deterministic (DSHA) approach; two spectra of unscaled natural accelerograms compatible with Fucino (Torre NS) and Colli Albani (Assisi EW) earthquake scenarios are also shown (modified from SABETTA 2014).
Fig. 7 – Spettri di riferimento impiegati per lo studio di microzonazione sismica dell'Area Archeologica Centrale di Roma ottenuto da studio probabilistico (INGV UHS) e deterministico (DSHA); sono inoltre mostrati gli spettri di due accelerogrammi reali non scalati compatibili con i terremoti di scenario Fucino (registrazione Torre NS) e Colli Albani (registrazione Assisi EW).

nical characteristics of the whole area (Fig. 2). 2D analyses were carried out on section #2 while additional 1D simulation were executed in relevant soil columns of the section. In the following the codes employed for the analyses and the methodology to include the uncertainty in dynamic soil properties of the anthropogenic unit are described.

5.1. 1D simulations

The 1D analyses were carried out with computer code Strata [KOTTKE and RATHJE, 2008]. The program performs equivalent linear site response analysis in the frequency domain using time domain input motions or random vibration theory (RVT) methods, and allows for randomization of the site properties. Nonlinear properties, layering thickness, shear-wave velocity, and depth to bedrock can be varied by the user in the analyses. An estimate of the seismic response of the 1D system and its standard deviation due to variations in the soil properties and layering is therefore made through Monte Carlo simulations. Monte Carlo methods compute the response of a system for different sets of imput parameters whose values are generated from assigned statistical distributions. Like for 2D analyses, a number of 20 simulations were carried out. However the stability of results were checked against statistics computed on 100 simulations.

In the present study, time series method was employed, *i.e.* acceleration time-history was provided as input motion. Moreover, soil layering (including bedrock) as well as dynamic properties of pre-anthropic units were kept fixed according to the values pertaining to the deterministic model. Only dynamic properties (V_S and nonlinear parameters) of anthropogenic cover unit were varied in the analyses.

In particular, the V_S at each layer of h lithotype was described by a log-normal distribution characterized by median value and standard deviation [TORO, 1995]. For each depth, these values were assigned on the basis of V_S profile in figure 6a showing statistics computed on V_S measurements carried out in the h unit. As a first approximation, the median values followed the exponential function in figure 6a while standard deviation was assumed constant with depth ($\sigma_{\ln Vs}$=0.24). For the inter-layer correlation between the shear-wave velocities, the factors proposed by TORO [1995] for a USGS class C deposit (V_{S30}=180-360 m/s) were employed.

Regarding the nonlinear behavior, the DARENDELI [2001] model, implemented in Strata, was used to describe the statistical distribution of soil properties; the variation is normal in distribution with standard deviation of both G/G0 and D curves varying with the magnitude of property according to the following equations:

$$\sigma_{GG_0} = \exp(-4.23) + \sqrt{\frac{0.25}{\exp(3.62)} - \frac{\left(\frac{G}{G_0} - 0.5\right)^2}{\exp(3.62)}}$$

$$\sigma_D = \exp(-5.0) + \exp(-0.25)\sqrt{D(\%)}$$

The model allowed to reproduce with satisfactory accuracy the average ± 1 standard deviation curves

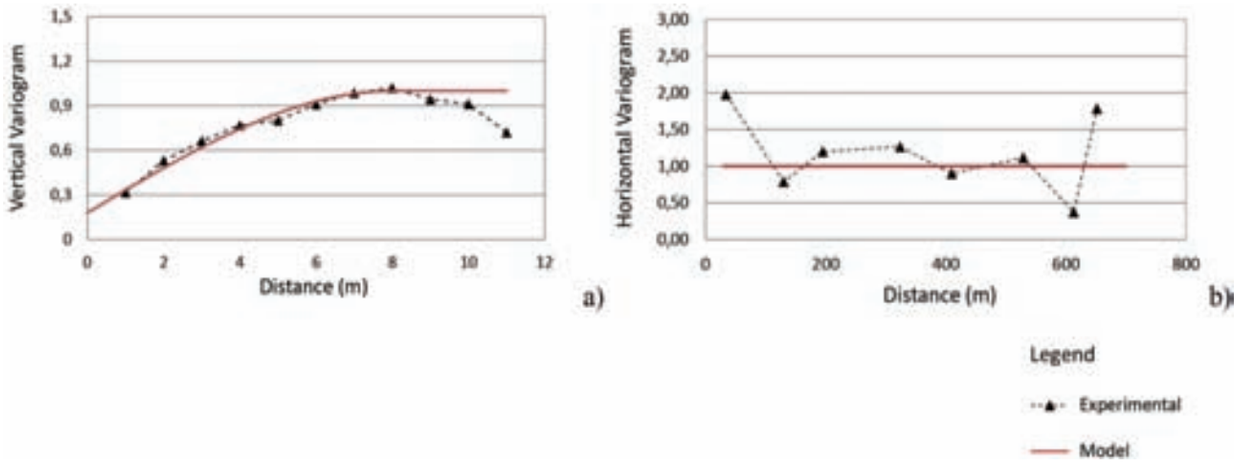

Fig. 8 – Vertical a) and horizontal b) variograms of Gaussian-transformed/detrended Vs data in h lithotype; see description in Tab. II.

Fig. 8 – Variogrammi verticali a) e orizzontali b) dei dati di V_S nel litotipo h dopo rimozione del trend e trasformazione in gaussiana; si veda descrizione in Tab. II.

proposed by ROLLINS *et al.,* [1998] for gravelly soils (Fig. 6b). At small strains the normal distribution was truncated to avoid values that are not physically possible (*i.e,* G/G_0 higher than 1 and D lower than 0%). The G/G_0 and D curves are not independent of each other because as the linearity of the soil increases, the damping (*i.e.*, the area inside the hysteresis loop) decreases. To capture this effect, the correlation coefficient ρ was set to - 0.5; because of the negative correlation, high normalized shear modulus values corresponds to low damping ratio values.

5.2. 2D simulations

The 2D numerical analyses were performed by using the finite element code QUAD4M [HUDSON *et al.,* 1994]; this numerical code operates in the time domain, incorporates a compliant base and uses an equivalent-linear procedure to model soil nonlinearity. In choosing the element size, the standard rule suggested by KUHLEMEYER and LYSMER [1973] was adopted to achieve a satisfactory level of solution accuracy; these authors define $h_{max}=V_S/(8\ fmax)$, where V_S = material shear wave velocity value selected accordingly to the shear strain level, h_{max} = maximum element height, and f_{max} =maximum frequency to be transmitted (assumed equal to 15 Hz). The finite element mesh consists of about 35'000 triangular-shaped elements. QUAD4M models geometric damping only at the bottom of the mesh by introducing viscous dampers (absorbing boundaries). In contrast, side boundaries are perfectly reflecting, and thus the side boundaries were extended about 200 m in both directions to reduce the influence of artificial reflected waves.

Both deterministic and stochastic 2D analyses were carried out. The deterministic analysis was executed by using the model reported in table I and figure 5; moreover for the anthropogenic unit the mean curves proposed by ROLLINS *et al.,* [1998] were employed. For the stochastic analyses, the nonlinear curves were kept fixed while simulations were run assuming the V_S distribution obtained from a number of 20 geostatistical simulations. In order to highlight the effects of uncertainties in dynamic properties of the anthropogenic unit, like for 1D analyses, V_S were varied only in this unit while deterministic values were employed for all other lithotypes.

The V_S geostatistical simulations were performed using the Sequential Gaussian Simulation (SGS), which is especially useful when the simulation mesh is not regular. The first step was to search for stationarity, which revealed a vertical trend, where Vs increses with depth. Horizontal and vertical variograms where then computed by using available geophysical test results in the h unit (16 in-hole tests for a total a 165 V_S measurements) after detrending and Gaussian transformation the corresponding data.

Results of the variability analysis of Vs in h unit are shown in table II while figure 8 shows the horizontal and vertical variograms that have been computed and modelled. With regard to the horizontal direction, it is interesting to observe in figure 8b which represents the horizontal variogram, that the range cannot be larger than 34 m (*i.e.*, the mean distance of the first point of the variogram). The availability of the data does not allow to define the effective range, which however has to be >0 m, for physical reasons. Nevertheless, a range in the order of some tens of meters is consistent both with the heterogeneity observed in the archaeological excavations and with the average size of the buried man-made structures.

Tab. II – Summary description of variographic analysis for h lithotype showing spatial correlation of Vs. The number in brackets represents the range/practical range of the variograms, in meters; the sign indicates the trend with depth (+: V_S increases with depth). As discussed in the text the range of the horizontal variogram has been chosen not through a fitting, but taking into account the heterogeneity of the anthropic cover and the average size of the buried man-made structures.
Tab. II – Descrizione delle analisi variografiche eseguite per il litotipo h riguardo la correlazione spaziale della V_S. Il numero tra parentesi indica il campo di variazione del variogramma (in metri) mentre il segno indica l'andamento con la profondità (+: V_S crescente con la profondità). Come discusso nel testo il campo di variazione del variogramma orizzontale è stato scelto non attraverso interpolazione dei dati sperimentali ma considerando l'eterogeneità della coltre antropica e la dimensione media delle strutture sepolte.

Lithotype	Trend	Vertical variogram	Horizontal variogram
h	yes (+)	1. Nugget 2. Spherical (8.0)	1. Spherical isotropic (30)

A total of 20 V_S distributions were computed in the h unit by SGS method honoring available V_S measurements along the in-hole profiles. More details about the procedure can be found in PAGLIAROLI *et al.,* [2014c] and references therein.

6. Numerical results from deterministic model

Numerical results were processed in terms of response spectra and Housner Intensity (HI) of the horizontal acceleration at ground surface. In order to cover the entire range of fundamental vibration periods pertaining to the archaeological remains and monuments in the area, HI was computed for three different period ranges: 0.1-0.5s, 0.5-1.0s, and 1.0-2.0s. The corresponding amplification factors profiles ($FH_{0.1\text{-}0.5s}$, $FH_{0.5\text{-}1.0s}$ and $FH_{1.0\text{-}2.0s}$) were then calculated by taking the ratio between the HI computed at the surface and the corresponding HI of the input motion.

FH amplification factors for cross-section #2 are reported in figure 9a. The three amplification factor ($FH_{0.1\text{-}0.5s}$, $FH_{0.5\text{-}1.0s}$, $FH_{1.0\text{-}2.0s}$) show quite different trends from both a qualitative and quantitative point of view, highlighting the "filter effect" that the soft rock and soil deposits exert on seismic motion (as a function of their mechanical and morphological features).

The amplification factor $FH_{0.1\text{-}0.5s}$ is almost constant on the Palatine hilltop (1.15 on average). No appreciable differences can be observed between the NW (multilayered deposit) and SE (FTR paleo-valley) sectors. Higher values (1.5-1.6) are observed in correspondence with the Labicano and Velabro alluvial valleys while significant deamplification occurs at the hill toe, especially in the NW sector (via di San Teodoro).

The significant ground motion amplification in the alluvial valleys is related to the impedance contrast between the soft layer formed by alluvial clays (SFTba3) plus anthropogenic deposits (h) and the underlying stiff soils (overconsolidated clays of the MVA and CIL1-FTR1 gravels). The seismic response is strongly 2D as clearly shown by the comparison between response spectra computed at node #A by 1D and 2D analyses (Fig. 9b). The 1D analyses significantly underestimate spectral ordinates especially around 0.2-0.3s where 2D resonance effects take place [PAGLIAROLI *et al.,* 2014b]. The minor fluctuations on the Palatine hilltop plateau indicating limited two-dimensional effects as confirmed by the overall agreement between 1D and 2D response spectra computed at node C (Fig. 9b). The low FH values computed at the hill toe can be ascribed to deamplification topographic effects, as observed in many experimental and numerical studies [PAGLIAROLI *et al.,* 2011).

The amplification factor $FH_{0.5\text{-}1.0s}$ has a maximum value (1.6-1.7) in correspondence with the FTR paleo-valley. Considering the shape ratio of the valley together with the mechanical properties of its fill deposits, 2D resonance phenomena can be excluded and the valley is mainly characterized by one-dimensional response even if the motion can be somewhat aggravated by surface waves generated at valley edge [PAGLIAROLI *et al.,* 2014b]. The response spectra computed at node #D from 2D and 1D analyses clearly show significant amplification with respect to the input spectrum in the 0.5-1.0 s range (Fig. 9b). Lower $FH_{0.5\text{-}1.0s}$ values occur in the Tiber alluvial valleys; these morphologic structures, characterized by minor size with respect to FTR valley, influence higher frequencies and thus, as seen previously, increase the motion in the 0.1-0.5s period range.

Finally, the factor $FH_{1.0\text{-}2.0s}$ shows minor fluctuations throughout the entire area, with limited amplification phenomena (1.25) only in the NW portion of the FTR paleo-valley (Fig. 9a).

7. Numerical results from stochastic models

Housner Intensity amplification factors FH computed for cross-section #2 assuming stochastic model for V_S distribution is shown in figure 10. For compari-

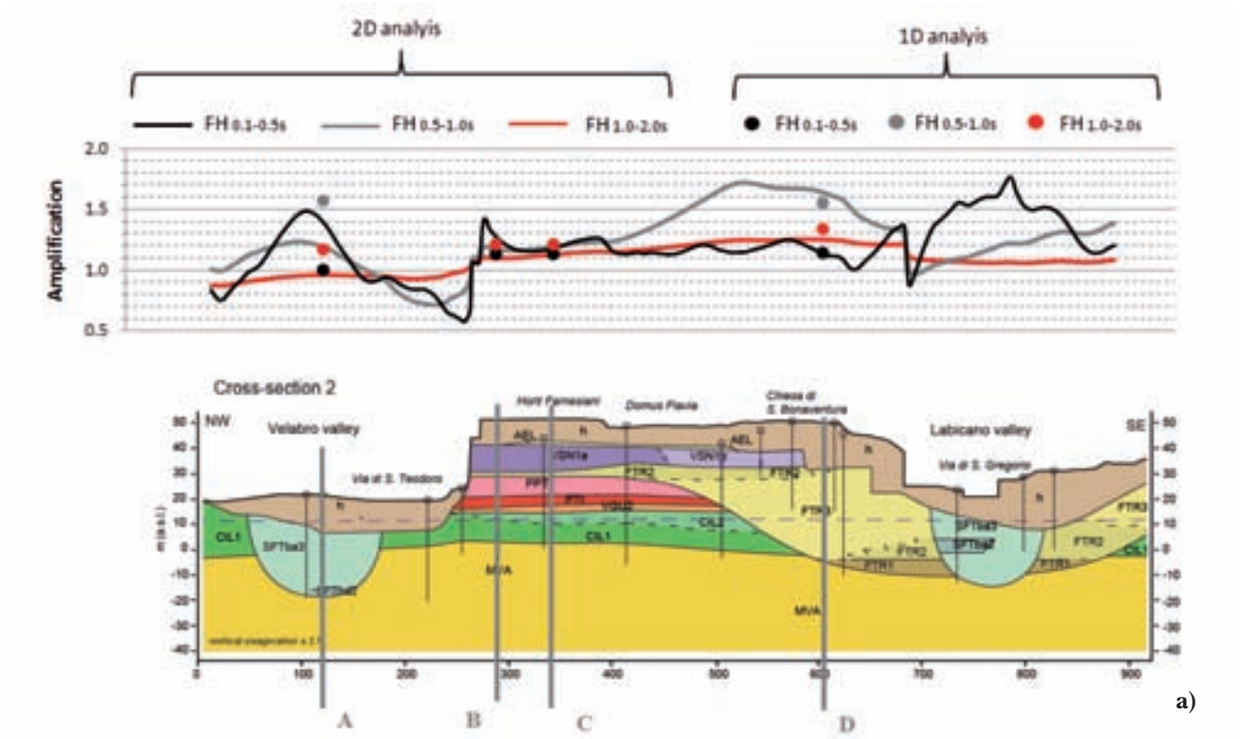

a)

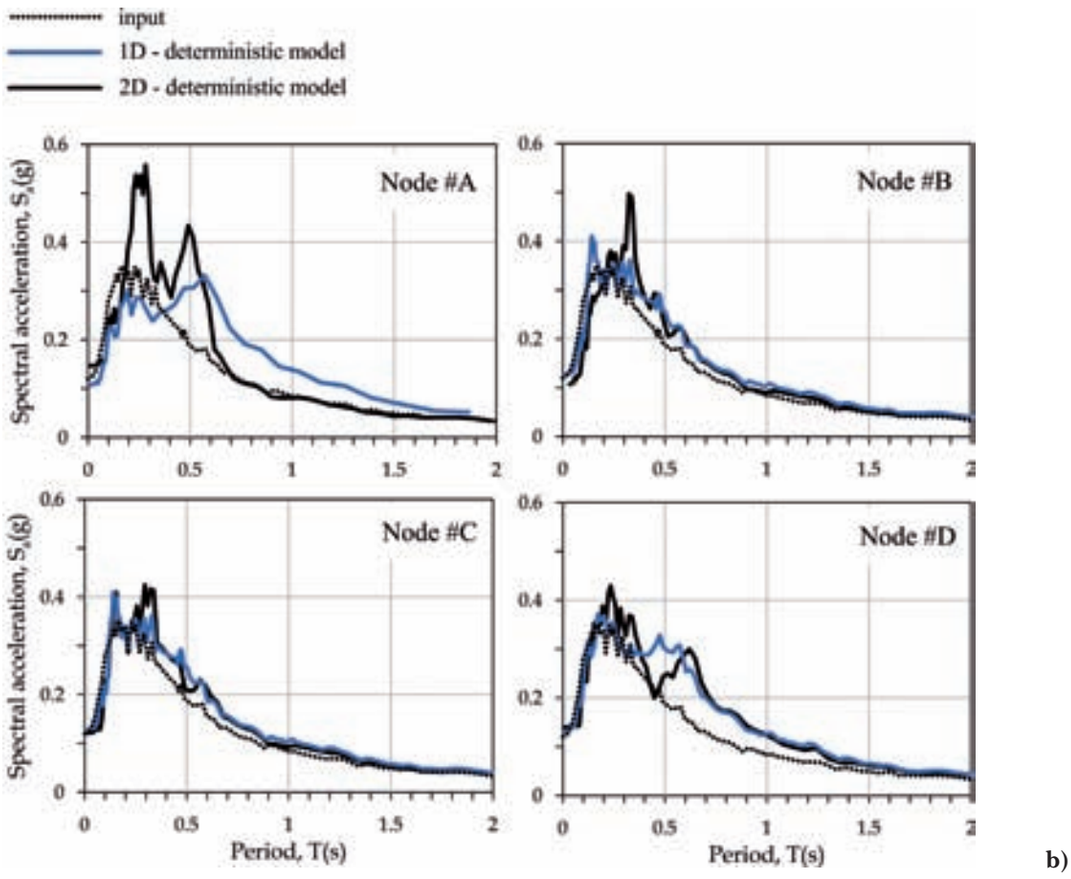

b)

Fig. 9 – Results of 1D and 2D analyses from deterministic model: Housner amplifications factors FH a) and response spectra at selected surface nodes b).

Fig. 9 – Risultati delle analisi 1D e 2D eseguite con modello deterministico: profili del fattori di amplificazione in termini di intensità di Housner FH a) e spettri di risposta in nodi rappresentativi in superficie b).

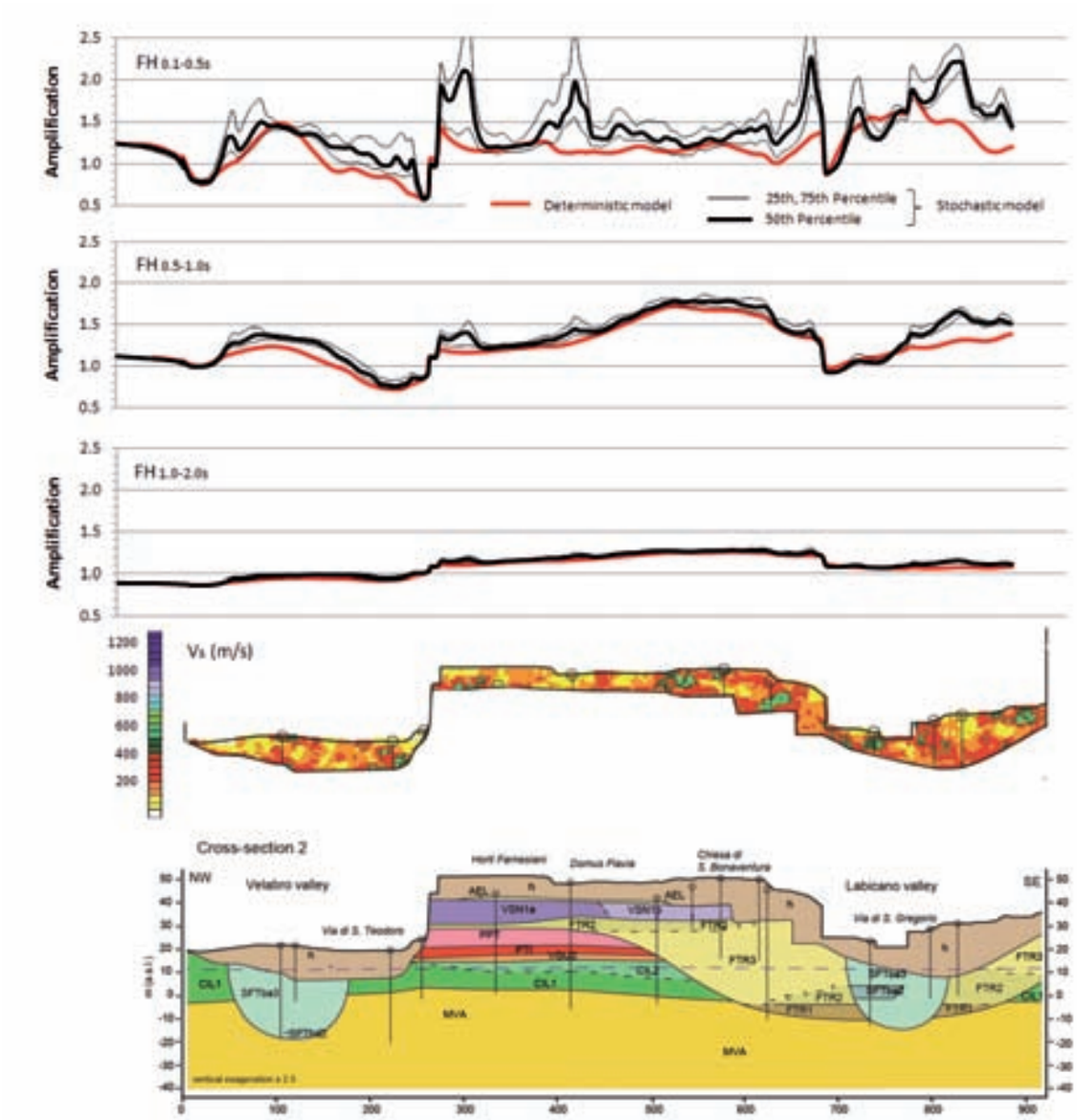

Fig. 10 – Housner amplifications factors FH profiles from 2D analyses carried out with deterministic and stochastic models; the profiles computed from stochastic model are represented in terms of 25th, 50th and 75th percentiles from 20 simulations. A representative V_S simulation in the h unit is also shown.

Fig. 10 – Profili del fattori di amplificazione in termini di intensità di Housner FH calcolati da analisi 2D eseguite con modello deterministico e stocastico; i risultati delle analisi stocastiche sono rappresentati in termini di 25°, 50° e 75° percentile calcolati sulle 20 simulazioni eseguite; a titolo di esempio è rappresentata una distribuzione di V_S all'interno dello strato h.

son the profiles obtained with the deterministic analysis were added. A representative distribution of shear wave velocity values in the anthropogenic layer from one of the V_S geostatistical simulation is also shown.

The FH profiles computed from stochastic model are represented in terms of 25th, 50th and 75th percentiles computed from the analyses carried out for the 20 simulations of V_S. The 50th percentile substantially agrees with the average values profile.

With reference to the 50th percentile an appreciable difference with the "deterministic" FH profiles can be observed only for the 0.1-0.5s period range (Fig. 10). Even if the general trend of FH is quite similar for both models, the 50th stochastic profiles can locally exceed more than 50% the deterministic amplification factors. This increment can reach about 100% if the reference is made to 75th percentile. Regarding the $FH_{0.5\text{-}1.0s}$ profile, minor differences between deterministic and stochastic results can be observed: even if reference is made to 75th percentile, the stochastic analyses exceed deterministic factors of 20% only in two areas (*i.e.* at hilltop NW

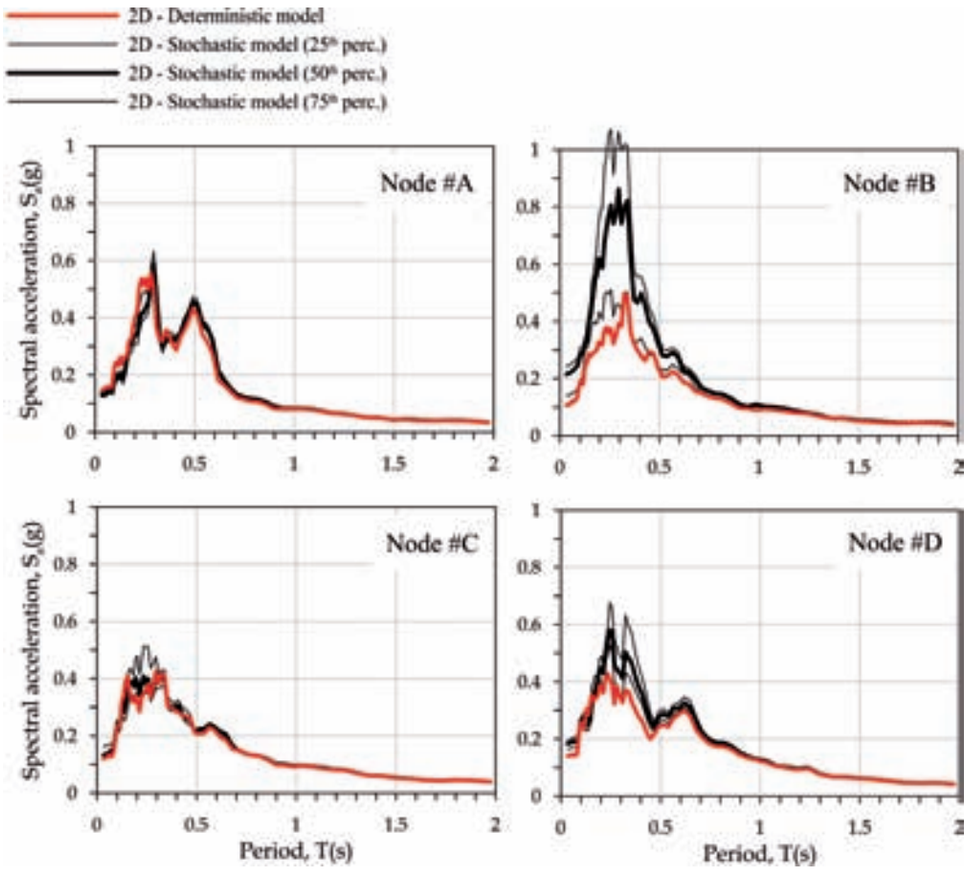

Fig. 11 – Response spectra computed in selected nodes (A-D see Fig. 9 for position) from 2D analyses carried out with deterministic and stochastic models; the spectra computed from stochastic model are represented in terms of 25th, 50th and 75th percentiles from 20 simulations.

Fig. 11 – Spettri di risposta calcolati in nodi rappresentativi (A-D si veda la Fig. 9 per l'ubicazione) da analisi 2D eseguite con modello deterministico e stocastico; gli spettri calcolati da analisi stocastiche sono rappresentati in termini di 25°, 50° e 75° percentile calcolati sulle 20 simulazioni eseguite.

edge and SE of the Labicano valley). No appreciable differences can be observed between deterministic and stochastic factors in the 1.0-2.0 s period range.

The same trend is shown by acceleration response spectra computed in selected nodes (Fig. 11). In general stochastic spectra are higher than those from deterministic simulations for period lower than 0.7s. In particular, at node #B, located at the progressive 300m along the cross section in which FH stochastic factors are well above deterministic values, 50th percentile maximum spectral ordinates are double of those computed with deterministic model.

This behaviour is coherent with the heterogeneities observed in the anthropic layer, and could be related to the complex 2D effects associated to waves scattered by the mechanical heterogeneities present in the stochastic model of h unit, greatly influencing high frequencies.

FH peaks provided by the stochastic model indeed roughly match the soft zones surrounded by more rigid materials (*i.e.*, masonry remains) in the anthropogenic cover (see the progressive 300 m and 400 m in Fig. 10). On the contrary, the small differences observed between deterministic and stochastic profiles in the 0.5-1.0 and 1.0-2.0s ranges are not surprising considering that the longer wavelengths associated to $FH_{0.5\text{-}1.0s}$ and $FH_{1.0\text{-}2.0s}$ are not influenced by short-range V_S variability in the h unit.

The relevant role played by lateral variations of V_s in the h unit is confirmed by looking at figures 9 and 12 in which the results of 1D and 2D results are compared for deterministic and stochastic analyses respectively. The stochastic analyses take into account the variation of V_S values (along vertical profile for 1D simulation in the space for 2D analyses) while the nonlinear properties were kept fixed according to ROLLINS *et al.*, [1998] average values. As general consideration, the dispersion associated to 2D simulation (quantified by 25th-75th percentile range) is higher in 2D case with respect to 1D simulation (Fig. 12). Moreover, it is interesting to note that at #B (at progressive of about 300 in section #2) as well

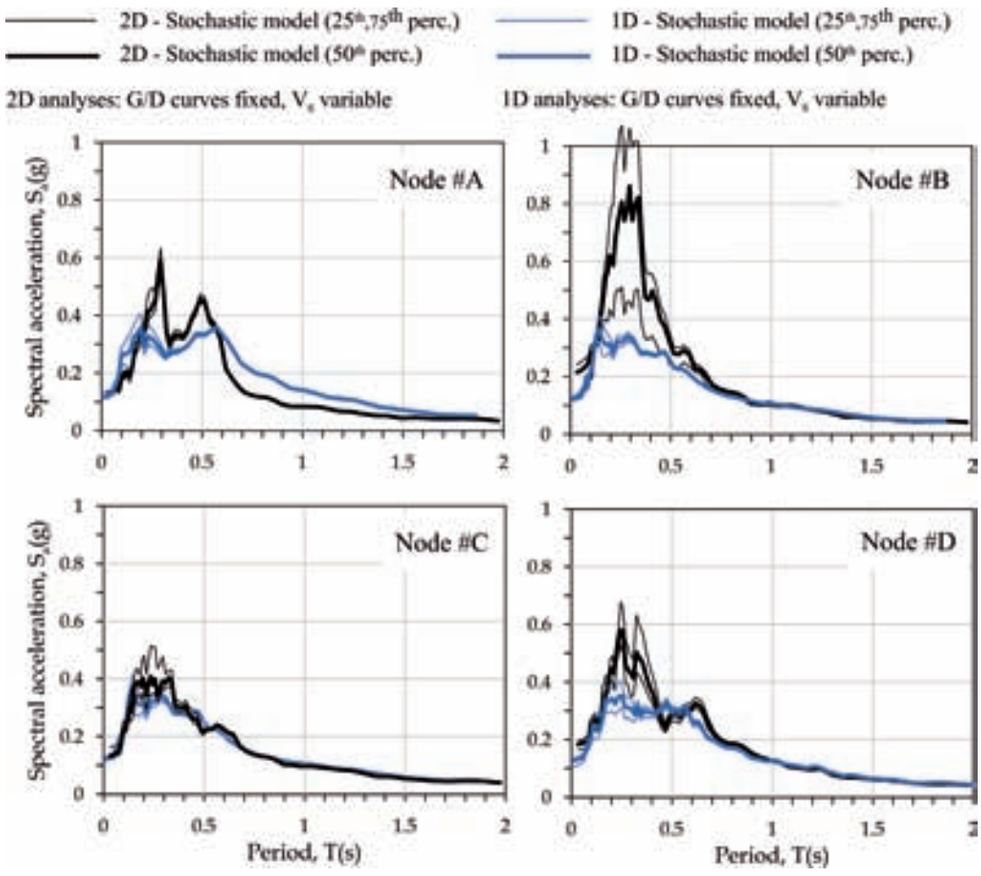

Fig. 12 – Response spectra computed in selected nodes (A-D see Fig. 9 for position) from 1D and 2D analyses carried out with stochastic model; the spectra are represented in terms of 25th, 50th and 75th percentiles from 20 simulations. In both 1D and 2D analyses nonlinear curves were kept fixed while V_S was variable.

Fig. 12 – Spettri di risposta calcolati in nodi rappresentativi (A-D si veda la Fig. 9 per l'ubicazione) da analisi 1D e 2D eseguite con modello stocastico; gli spettri sono rappresentati in termini di 25°, 50° e 75° percentile calcolati sulle 20 simulazioni eseguite. Sia nelle analisi 1D che in quelle 2D le curve delle proprietà non lineari sono state mantenute fisse mentre è stata variata la V_S.

at #D (progressive 600 m) the difference between 2D and 1D simulation is much higher for stochastic simulations than for deterministic ones. This means that in stochastic simulations "additional" 2D effects related to V_S spatial heterogeneity, considered only by 2D simulation, do occur. The difference between 1D and 2D seismic response is not significantly enhanced by stochastic simulations in node #A and #C. At node #A this probably occurs because the seismic response is essentially driven by 2D resonance of clayey valley underlying the h unit and the role of anthropogenic cover is therefore less relevant.

The effect of uncertainty in nonlinear properties was investigated by means of 1D stochastic analyses. As explained before, the normalized shear modulus and damping curves were varied in the average ± one standard deviation ranges proposed by ROLLINS *et al.* [1998] while V_S profile was kept fixed according to the gradient expressed by the fitting curve in figure 6a. The response spectra at nodes #A-D (Fig. 13) show no appreciable dispersion in the seismic response due to variation in dynamic curves being the 25th percentile almost coincident with the 75th one. On the contrary is more pronounced, even if to a less extent with respect to 2D conditions, the role of variation of V_S profile. This behavior could be explained by the moderate nonlinearity degree experienced by the soils being the maximum shear strain amplitude in the h unit in the order of 0.02 % on average in 1D conditions.

8. Discussion and conclusions

The results of a numerical study aimed at the evaluation of the seismic response of the Central Archaeological Area of Rome including Palatine hill, Roman Forum, and Coliseum is presented in this paper. A large amount of data, collected from previous investigations and derived from ad hoc geotechnical-geophysical survey, allowed to define an integrate subsoil model for site response numerical modeling. For the definition of the subsoil model particu-

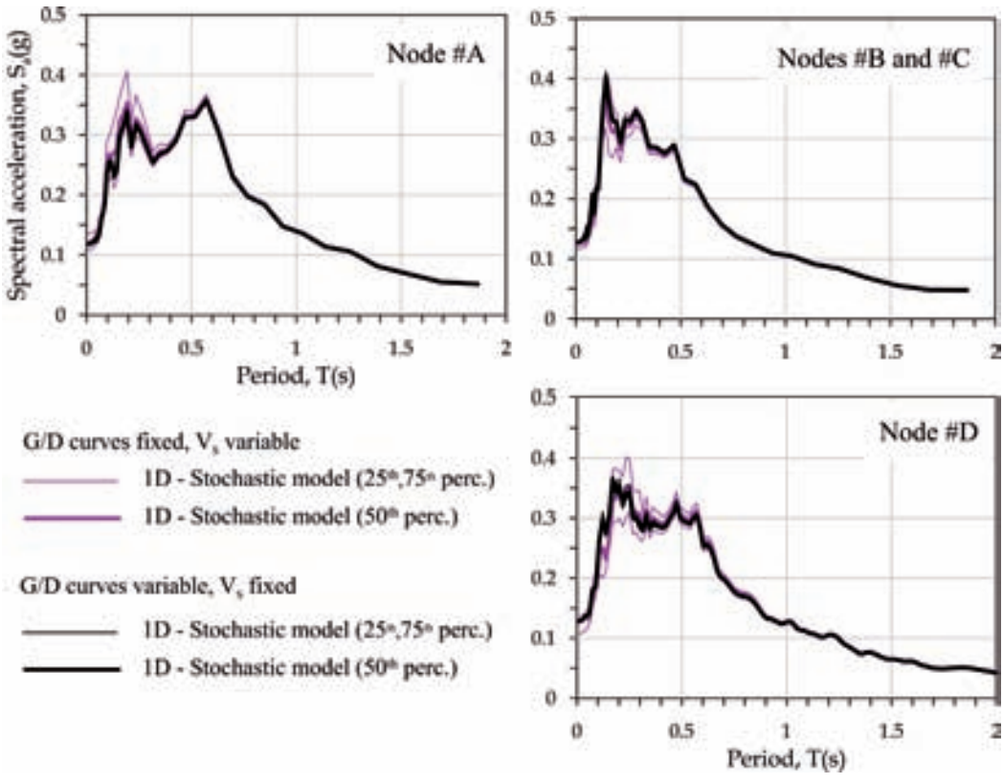

Fig. 13 – Response spectra computed in selected nodes (A-D see Fig. 9 for position) from 1D analyses carried out with stochastic model; the spectra are represented in terms of 25th, 50th and 75th percentiles from 20 simulations. Results obtained with V_S variable and nonlinear properties fixed are compared with those derived from varying non linear properties with V_S fixed.
Fig. 13 – Spettri di risposta calcolati in nodi rappresentativi (A-D si veda la Fig. 9 per l'ubicazione) da analisi 1D eseguite con modello stocastico; gli spettri sono rappresentati in termini di 25°, 50° e 75° percentile calcolati sulle 20 simulazioni eseguite. I risultati ottenuti tendo fisse le curve delle proprietà non lineari e variando le V_S sono confrontati con quelli ottenuti variando le curve non lineari e mantenendo costante la V_S.

lar efforts were devoted to the characterization of the buried morphology and mechanical properties of the anthropogenic cover. Its thickness reaches 20 m and therefore strongly controls the seismic response in the moderate-to -high frequency range. This layer is constituted by "dominant masonry" and "dominant infill" zone strongly variable in the space thus exhibiting wide spatial heterogeneity in dynamic properties.

A uniform hazard spectrum with return period of 475 years was selected as reference spectrum and a simulated spectrum-compatible time-history acceleration was employed for input motion. Bi-dimensional numerical analyses were then carried out for one representative cross-sections while additional 1D simulation were executed in relevant soil columns of the same section.

The results of 1D and 2D analyses carried out with a deterministic model (i.e assuming "average" properties in all lithotypes including the anthropogenic unit) show that ground motion distribution is mainly controlled by 1D resonance phenomena mainly associated to anthropogenic cover and 2D effects associated with i) recent alluvial valleys bordering Palatine hill, and ii) a large and deep N-S oriented paleo-valley.

Moreover, in order to investigate the effect of the uncertainty and heterogeneity in dynamic soil properties of the anthropogenic unit, 1D and 2D stochastic analyses were carried out.

Regarding the V_S profiles, S-wave velocity distributions compatible with values measured at in-hole profiles were first generated from twenty 2D geostatistical simulations. Numerical results obtained from 2D stochastic simulations were then compared with those from the deterministic model.

Appreciable difference can be observed in the 0.1-0.5s period range: the general trend of Intensity Housner amplification factors (FH) is quite similar for both subsoil models but FH from stochastic simulations can locally exceed of about 50% on average the deterministic amplification factors. This increment can reach about 100% if the reference is made to maximum spectral ordinates of response spectra. Waves scattering phenomena due to mechanical heterogeneities in the anthropogenic cover could explain the ground motion aggravation.

Regarding the nonlinear properties (*i.e.* normalized shear modulus and damping curves), the stochastic analyses were carried only in 1D conditions. The

results showed that in moderate seismicity areas like that under study (i.e. input PGA at bedrock of about 0.1g) the role of uncertainties in nonlinear properties is negligible with respect to that associated to V_S spatial uncertainty. This is because the moderate nonlinearity experienced by the soils (maximum shear strain amplitude of the order of 0.02 % on average).

The case study here presented shows how the strong heterogeneity of shallow geological bodies, like thick anthropogenic cover in archaeological or ancient urbanized areas, can influence the result of the site response studies, at least in the medium to high frequency range.

This heterogeneity conditions the geometry and distribution of zones in microzonation studies and the seismic action to be used for structural design or seismic retrofitting.

Under these conditions, therefore, the results of analyses carried out with a deterministic subsoil model using "average values" should be employed carefully, and the use of methods taking into account spatial variability of V_S is encouraged.

References

ANDRADE J.E., BORJA R.I. (2006) – *Quantifying sensitivity of local site response models to statistical variations in soil properties*. Acta Geotechnica,1, pp. 3-14.

ANSAL A., TÖNÜK G., KURTULUS A. (2009) – *Microzonation for Urban Planning*. In: Tankut AT (Ed.) "Earthquakes and Tsunamis, Geotechnical, Geological, and Earthquake Engineering", 11, pp. 133-152.

BAZZURRO P., CORNELL A. (2004) – *Ground-motion amplification in nonlinear soil sites with uncertain properties*. Bull. Seismol. Soc. Am., 94, n.6, pp. 2090-2109.

CECCHI R. (2010) – *Roma Archæologia. Interventi per la tutela e la fruizione del patrimonio archeologico*. Secondo rapporto, Mondadori Electa, Milano.

CECCHI R. (2011) – *Roma Archæologia. Interventi per la tutela e la fruizione del patrimonio archeologico*. Terzo rapporto, vol. II, Mondadori Electa, Milano.

CHILES J.P., DELFINER P. (1999) – *Geostatistics: modeling spatial uncertainty*. Wiley, New York.

DARENDELI M. B. (2001) – *Development of a new family of normalized modulus reduction and material damping curves*. PhD Dissertation, Austin, The University of Texas.

FACCIOLI E. (1976) – *A stochastic approach to soil amplification*. Bull. Seismol. Soc. Am., 66, n. 4, pp. 1277-91.

FUNICIELLO R., GIORDANO G. (2008) – *Note illustrative della Carta Geologica d'Italia alla scala 1:50.000, Foglio 347 Roma*. APAT-Servizio Geologico d'Italia, Roma.

GALLI P., MOLIN D. (2014) – *Beyond the damage threshold: the historic earthquakes of Rome*. Bulletin of Earthquake Engineering, 12, pp. 1277-1306.

HATANAKA M., SUZUKI Y., KAWASAKI T., ENDO M. (1988) – *Cyclic undrained shear properties of high quality undisturbed Tokyo gravel*. Soils and Foundations, 28, n. 4, pp. 57-68.

HUDSON M., IDRISS I.M., BEIKAE M. (1994) – *QUAD4M: a computer program to evaluate the seismic response of soil structures using finite element procedures and incorporating a compliant base*. Dpt. of Civil and Environmental Eng., Univ. of California Davis, Davis, California.

IDRISS I.M. (2004) – *Evolution of the state of practice*. Int. Workshop on the "Uncertainties in Nonlinear Soil Properties and Their Impact on Modeling Dynamic Soil Response", Pacific Earthquake Engineering Research Center, Richmond, California.

KOTTKE A.R., RATHJE E.M. (2008) – *Technical manual for Strata*. University of California, Berkeley.

KUHLEMEYER R.L., LYSMER J. (1973) – *Finite element method accuracy for wave propagation problems*. Journal of Soil Mechanics and Foundation Division, ASCE, 99(SM5), pp. 421- 427.

MANCINI M., MARINI M., MOSCATELLI M., PAGLIAROLI A., STIGLIANO F., DI SALVO C., SIMIONATO M., CAVINATO G.P., CORAZZA A. (2014) – *A physical stratigraphy model for seismic microzonation of the Central Archaeological Area of Rome (Italy)*. Bull. Earthquake Eng., 12, pp. 1339-1363.

MOSCATELLI M., PAGLIAROLI A., MANCINI M., STIGLIANO F., CAVUOTO G., SIMIONATO M., PERONACE E., QUADRIO B., TOMMASI P., CAVINATO G.P. ET AL (2012) – *Integrated subsoil model for seismic microzonation in the Central Archaeological Area of Rome (Italy)*. Disaster Adv, 5, pp. 109-124.

MOSCATELLI M., PAGLIAROLI A., CAVINATO G. P., CASTENETTO S., NASO G. (2014a) – *Seismic microzonation of Palatine hill, Roman Forum and Coliseum Archeological Area*. Bulletin of Earthquake Engineering, 12, pp. 1269-1275.

MOSCATELLI M., PISCITELLI S., PIRO S., STIGLIANO F., GIOCOLI A., ZAMUNER D., MARCONI F. (2014b) – *Integrated geological and geophysical investigations to characterized the anthropic layer of the Palatine hill and Roman Forum (Rome, Italy)*. Bull. Earthquake Eng., 12, pp. 1319-1338.

MUCCIARELLI M., SPINELLI A., PACOR F. (2004) – *Un programma per la generazione di accelerogrammi sintetici "fisici" adeguati alla nuova normativa*. 11° Congresso Nazionale l'Ingegneria Sismica in Italia, Genova 25-29 gennaio 2004.

PAGLIAROLI A., LANZO G., D'ELIA B. (2011) – *Numerical evaluation of topographic effects at the Nicastro ridge in Southern Italy*. Journal of Earthquake Engineering, 15, n. 3, pp. 404-432.

PAGLIAROLI A., LANZO G., TOMMASI P., DI FIORE V. (2014a) – *Dynamic characterization of soils and soft rocks of the Central Archaeological Area of Rome*. Bulletin of Earthquake Engineering, 12, pp. 1365-1381.

PAGLIAROLI A., QUADRIO B., LANZO G., SANÒ T. (2014b) – *Numerical modelling of site effects in the Palatine hill, Roman Forum and Coliseum archaeological area*. Bulletin of Earthquake Engineering, 12, pp. 1383-1403.

Pagliaroli A., Moscatelli M., Raspa G., Naso G. (2014c) – *Seismic microzonation of the Central Archeological Area of Rome: results and uncertainties*. Bulletin of Earthquake Engineering, 12, pp. 1405.1428.

Pensabene P. (2001) – *L'interpretazione delle evidenze archeologiche alla luce dei miti di fondazione*. In: Pensabene P. Falzone S. (Eds.) *Scavi del Palatino I. L'area sud-occidentale del Palatino tra l'età protostorica e il IV secolo a.C. Scavi e materiali della struttura ipogea sotto la cella del tempio della Vittoria*, L'Erma di Bretschneider, Roma, pp. 3-19.

Rathje E. M., Kottke A. R., Trent W. L. (2010) – *Influence of input motion and site property variabilities on seismic site response analysis*. Journal of Geotechnical and Geoenvironmental Engineering, 136, n. 4, pp. 607-619.

Rollins, K. M., Evans, M. D., Diehl, N. B., Daily III, W. D. (1998) – *Shear modulus and damping relationships for gravels*. Journal of Geotechnical and Geoenvironmental Engineering, 124, n. 5, pp. 396-405.

Rota, M., Lai C. G., Strobbia C. L. (2011) – *Stochastic 1D site response analysis at a site in central Italy*. Soil Dynamics and Earthquake Engineering, 31, n. 4, pp. 626-639.

Sabetta F. (2014) – *Seismic hazard and design earthquakes for the Central Archaeological Area of Rome*. Bulletin of Earthquake Engineering, 12, pp. 1307-1317.

Signorini R. (1939) – *Risultati geologici della perforazione eseguita dall'AGIP alla mostra autarchica del minerale nel Circo Massimo di Roma*. Bollettino della Società Geologica Italiana, 58, pp. 60-63 (in Italian).

Tomei M.A., Filetici M.G. (2011) – *Domus Tiberiana. Scavi e restauri 1990-2011*. Mondadori Electa, Milano.

Toro G. R. (1995) – *Probablistic models of site velocity profiles for generic and site-specific ground-motion amplification studies*. Upton, New York, Brookhaven National Laboratory.

Effetti dell'incertezza e dell'eterogeneità dei terreni sulla risposta sismica di aree archeologiche: un caso di studio

Sommario

L'articolo riporta i risultati di uno studio numerico volto alla valutazione della risposta sismica dell'Area Archeologica Centrale di Roma comprendente Palatino, Foro Romano e Colosseo. Un ruolo rilevante è svolto dalla morfologia sepolta e dalle proprietà meccaniche dello strato antropico che raggiunge uno spessore massimo di 20 m. Questo strato è costituito da zone a "muratura dominante" e zone a "interro dominante" che si alternano nello spazio dando luogo a una forte variabilità spaziale delle proprietà dinamiche la cui ricostruzione è affetta da notevoli incertezze. Per studiare gli effetti di tale incertezza sul moto sismico in superficie, sono state eseguite analisi stocastiche 1D e 2D. I risultati numerici sono stati poi confrontati con quelli ottenuti da un modello deterministico definito utilizzando valori "medi" delle proprietà dinamiche.

L'influenza delle incertezza nella distribuzione della velocità delle onde di taglio e nelle proprietà non lineari dello strato antropico (espresse in termini di curve del modulo di taglio normalizzato e dello smorzamento) viene evidenziata in termini di profili dei fattori di amplificazione dell'intensità Housner e di spettri di risposta dell'accelerazione in nodi significativi in superficie.